Biochimica et Biophysica Acta 1807 (2011) 458–469

Contents lists available at ScienceDirect

Biochimica et Biophysica Acta

journal homepage: www.elsevier.com/locate/bbabio

Mitochondria–cytoskeleton interaction: Distribution of β-tubulins in cardiomyocytes and HL-1 cells

Rita Guzun [a], Minna Karu-Varikmaa [b], Marcela Gonzalez-Granillo [a], Andrey V. Kuznetsov [c], Lauriane Michel [a], Cécile Cottet-Rousselle [a], Merle Saaremäe [b], Tuuli Kaambre [b], Madis Metsis [b], Michael Grimm [c], Charles Auffray [a,d], Valdur Saks [a,b,*]

[a] INSERM U884, Laboratory of Fundamental and Applied Bioenergetics, Joseph Fourier University, Grenoble, France
[b] Laboratory of Bioenergetics, National Institute of Chemical Physics and Biophysics, Tallinn, Estonia
[c] Cardiac Surgery Research Laboratory, Department of Heart Surgery, Innsbruck Medical University, Innsbruck, Austria
[d] Functional Genomics and Systems Biology for Health, CNRS Institute of Biological Sciences, Villejuif, France

ARTICLE INFO

Article history:
Received 30 November 2010
Received in revised form 13 January 2011
Accepted 31 January 2011
Available online 4 February 2011

Keywords:
Cardiomyocytes
Creatine kinase
HL-1 cells
Mitochondrial interactosome
β-tubulin isotypes
Warburg effect

ABSTRACT

Mitochondria–cytoskeleton interactions were analyzed in adult rat cardiomyocytes and in cancerous non-beating HL-1 cells of cardiac phenotype. We show that in adult cardiomyocytes βII-tubulin is associated with mitochondrial outer membrane (MOM). βI-tubulin demonstrates diffused intracellular distribution, βIII-tubulin is colocalized with Z-lines and βIV-tubulin forms microtubular network. HL-1 cells are characterized by the absence of βII-tubulin, by the presence of bundles of filamentous βIV-tubulin and diffusely distributed βI- and βIII-tubulins. Mitochondrial isoform of creatine kinase (MtCK), highly expressed in cardiomyocytes, is absent in HL-1 cells. Our results show that high apparent K_m for exogenous ADP in regulation of respiration and high expression of MtCK both correlate with the expression of βII-tubulin. The absence of βII-tubulin isotype in isolated mitochondria and in HL-1 cells results in increased apparent affinity of oxidative phosphorylation for exogenous ADP. This observation is consistent with the assumption that the binding of βII-tubulin to mitochondria limits ADP/ATP diffusion through voltage-dependent anion channel of MOM and thus shifts energy transfer via the phosphocreatine pathway. On the other hand, absence of both βII-tubulin and MtCK in HL-1 cells can be associated with their more glycolysis-dependent energy metabolism which is typical for cancer cells (Warburg effect).

1. Introduction

Recent advances in studies of cellular energetics show that the mechanisms of regulation of energy fluxes and respiration in cells *in vivo* can be understood only in the framework of molecular system bioenergetics, which considers energy metabolism not only as a network of biochemical reactions, but also takes into account the spatial organization and temporal dynamics of intracellular interactions [1–4]. Interactions between cellular components result in appearance of new, system level properties such as macro- and micro-compartmentation of metabolites, metabolic channeling and functional coupling [3–7]. Thus, they give rise to specific mechanisms, such as energy transfer from the mitochondria to the cytoplasm through phosphotransfer networks [3–9].

Among the factors, most important for regulation of mitochondrial function in the cells *in vivo*, are the interactions of these organelles with other cellular structures, such as the cytoskeleton [10–13]. Among the cytoskeleton structures, one of the most important roles is attributed to the tubulin–microtubular system. Interactions of mitochondria with tubulin have been observed by many authors [14–18]. The most detailed and pioneering study of the structural interactions performed by Saetersdal et al. in 1990 demonstrated the presence of immunogold anti-β-tubulin labeling at the mitochondrial outer membrane (MOM) in cardiomyocytes, as well as in fibers in close apposition to this membrane [18]. For 20 years, this important observation was left almost unnoticed and unexplained. A possible functional role of this mitochondria-associated tubulin was found in extensive studies of the respiration regulation in permeabilized cells (i.e. *in situ* mitochondria [19]), when it has been shown that the apparent K_m for ADP in oxidative muscle cells (cardiomyocytes, skeletal m. soleus) is 20–30 times higher than in isolated mitochondria [8,20–23]. In addition, the high apparent K_m for ADP was found to be decreased by addition of creatine to activate MtCK [21,22], or by proteolytic treatment [23]. The apparent K_m for exogenous ADP is indicative of the availability of ADP for the adenine nucleotide translocase (ANT) in the mitochondrial inner membrane (MIM) and was proposed to be dependent on the permeability of the voltage-dependent anion channel (VDAC) located in the (MOM) [11,12]. The

* Corresponding author at: Laboratory of Bioenergetics, Joseph Fourier University, 2280, Rue de la Piscine, BP53X-38041, Grenoble Cedex 9, France.
E-mail address: Valdur.Saks@ujf-grenoble.fr (V. Saks).

0005-2728/$ – see front matter © 2011 Elsevier B.V. All rights reserved.
doi:10.1016/j.bbabio.2011.01.010

strong decrease of the apparent K_m for exogenous ADP induced by trypsin pointed to the possible involvement of some cytoskeleton-related protein(s) in the control of the VDAC permeability originally referred to as "factor X" [11,12,24]. Using immunofluorescence confocal microscopy Appaix et al. showed that tubulin and plectin are among cytoskeletal proteins sensitive to the proteolytic treatment [24]. The first established candidate for the role of "factor X" proved to be αβ heterodimeric tubulin, which strongly modulated the VDAC conductance upon binding to channel's protein reconstructed into a planar lipid membrane [17]. Reconstitution experiments indicated that the addition of the heterodimeric tubulin to isolated mitochondria strongly increased the apparent K_m for ADP [16].

The results of these experimental studies led to the assumption that oxidative phosphorylation in cardiomyocytes is effectively regulated by the mitochondrial interactosome (MI), a supercomplex consisting of the ATP synthasome, mitochondrial creatine kinase (MtCK), VDAC, tubulin controlling VDAC permeability, and possible linker proteins localized in the contact sites of two mitochondrial membranes [8,25,26].

Pedersen et al. have shown the existence of a similar supercomplex in cancer cells containing the ATP synthasome-VDAC-Hexokinase 2 [27–29]. In contrast to the highly oxidative phenotype of metabolism characteristic for adult cardiomyocytes, cancer cells have a glycolytic phenotype characterized by the increased lactic acid production even in the presence of sufficient amounts of oxygen to support mitochondrial function [30–32]. This common metabolic hallmark of malignant tumors was discovered by Otto Warburg and is known as the "Warburg effect" [33,34]. Our earlier studies of mouse cancerous HL-1 cells of cardiac phenotype have shown that the apparent K_m for exogenous ADP is very low and creatine has no effect on their respiration [35,36]. These functional properties of HL-1 cells appear related to alterations in the structure of the mitochondrial interactosome [8,36,37].

In the present work, we continue this direction of research by comparative study of the intracellular distribution of different isotypes of tubulin in normal adult cardiomyocytes and HL-1 cells, using confocal fluorescence and immunofluorescence microscopy and Western blotting. We show that the localization and functional role of β-tubulin isotypes are different in oxidative muscle tissues and HL-1 cells. Most importantly, in adult cardiomyocytes we identified an isotype of tubulin which is associated with mitochondria–βII-tubulin. The absence of this isotype in cancer cells appears to allow binding of hexokinase 2 to VDAC and to be directly involved in development of the Warburg effect.

2. Materials and methods

2.1. Cells preparation

For this study we used freshly isolated adult rat cardiomyocytes, isolated rat heart mitochondria and non-beating cancerous HL-1 cells of cardiac phenotype developed in Dr. W.C. Claycomb laboratory (Louisiana State University Health Science Center, New Orleans, LA, USA).

2.2. Isolation of adult cardiac myocytes

Adult cardiomyocytes were isolated after perfusion of the rat heart with collagenase using modified technique described previously [21]. Wistar male rats (300–350 g) were anaesthetized with pentobarbital and blood was protected against coagulation by injection of 500 U of heparin. The heart was quickly excised preserving a part of the aorta and placed into isolation medium (IM) of the following composition: 117 mM NaCl, 5.7 mM KCl, 4.4 mM $NaHCO_3$, 1.5 mM KH_2PO_4, 1.7 mM $MgCl_2$, 11.7 mM glucose, 10 mM creatine, 20 mM taurine, 10 mM PCr, 2 mM pyruvate and 21 mM HEPES, pH 7.1. The excised rat heart was cannulated by the aorta and suspended in a Langendorf system for perfusion and washed for 5 min with a flow rate of 15–20 ml/min. The collagenase treatment was performed by switching the perfusion to circulating isolation medium supplemented with 0.03 mg/ml collagenase (Roche) and BSA 2 mg/ml at the flow rate of 5 ml/min for 20–30 min. The end of the digestion was determined following the decrease in perfusion pressure measured by a manometer. After the digestion, the heart was washed with IM for 2–3 min and transferred into IM containing 20 μM $CaCl_2$, 10 μM leupeptin, 2 μM soybean trypsin inhibitor (STI) and 2 mg/ml fatty acid free BSA. The cardiomyocytes were then gently dissociated using forceps and pipette suction. Cell suspension was filtered through a crude net to remove tissue remnants and let to settle for 3–4 min at room temperature. After 3–4 min the initial supernatant was discarded, pellet of cardiomyocytes resuspended in 10 ml of IM containing 20 μM $CaCl_2$ and the protease inhibitors. This resuspension–sedimentation cycle with calcium-tolerant cells was performed twice, after that cardiomyocytes were gradually transferred from 20 μM Ca^{2+} IM into free calcium Mitomed (supplemented with protease inhibitors and BSA) and washed 5 times. Each time, slightly turbid supernatant was removed after 4–5 min of the cells' sedimentation. Isolated cells were re-suspended in 1–2 ml of Mitomed solution [19] for the labeling with MitoTracker fluorophore or in paraformaldehyde 4 % for fixation.

2.3. Isolation of mitochondria from cardiac muscle

Heart mitochondria were isolated from adult white Wistar rats 300 g body weight, as described by Saks et al. 1975 [58]. The rats were anesthetized with intraperitoneal injection of Pentobarbital (50 mg/kg body weight). Hearts were removed and placed into ice-cold isolation medium containing 300 mM sucrose, 10 mM HEPES, pH 7.2, and 0.2 mM EDTA. Atriums and vessels were cut off and the ventricles finely minced by scissors. After a brief mild homogenization in a glass potter with teflon pestle (clearance 0.7–0.8) at 200 rpm, during 30 sec, tissue underwent proteolytic digestion in the presence of 0.125 mg/ml trypsin for 15 min at 4 °C. The proteolysis was stopped by addition of 0.5 mg/ml soybean trypsin inhibitor (STI). The sample was carefully and briefly homogenized in a glass-teflon homogenizer (clearance 0.7–0.8) at 250 rpm and 4 °C. This homogenization was followed by a second one (300 rpm, 4 °C) using the potter with smaller clearance. After, the homogenate was centrifuged at 1250*g* for 10 min at 4 °C. The supernatant was carefully separated and centrifuged at 6300*g* for 10 min at 4 °C. Mitochondrial pellet obtained was re-suspended in 15 ml of ice-cold extraction medium, supplemented with 1 mg/ml fatty acid free bovine serum albumin, BSA, and washed three times applying the principle of differential centrifugation (3800*g* at 4 °C for 10 min each time), always carefully removing the upper layer of light fraction of damaged mitochondria in the pellet if it was present [38]. The final pellet containing mitochondria was re-suspended in 1 ml of the same isolation medium.

2.4. Cell culture

Cardiac muscle cell line, designated as HL-1 cells were derived in the Claycomb laboratory from the AT-1 mouse atrial cardiomyocyte tumor lineage [35–37]. Non-beating HL-1 cells (NB HL-1) were obtained from the HL-1 line developed by W. Claycomb by growing them up in different serum (Gibco fetal bovine serum) [35–37]. NB HL-1 cells do not beat spontaneously. These cells maintain cardiac properties characterized by immunolabeling actin, tubulin, desmin, connexin 43, myosin (developmental isoform), dihydropyridine receptors, by the presence of a sodium–calcium exchanger [36,37]. These cells are devoid of sarcomere structures and possess randomly organized filamentous dynamic mitochondria. NB HL-1 possess the electrophysiological characteristics and ionic currents of cardiac cells

(cardiac potassium current), but do not display electrical pacemaker activity and do not show spontaneous depolarization [36].

HL-1 cells were cultured in fibronectin (12.5 mg/l)–gelatine (0.02%) coated flasks containing Claycomb medium (Sigma) supplemented with 10% foetal bovine serum (PAN Biotech GmbH), 2 mM L-glutamine (PAN Biotech GmbH), 0.1 mM norepinephrine (Sigma), ascorbic acid 0.3 mM (Sigma), 100 U/ml penicillin and 100 μg/ml streptomycin (Sigma) in a humid atmosphere of 5% CO2 / 95% air at 37 °C. Cells were cultured in Lab-Tek® chambered coverglass, chamber volume 0.5 ml.

2.5. Sample preparation for Western blot analysis

Male Wistar rats (300–350 g) were anesthetized with pentobarbital, de-coagulated using 500 U heparin and decapitated. Approximately 50 mg samples of the brain tissue were quickly removed, weighed in cryovials and frozen in liquid nitrogen. At the same time, heart was quickly excited, ca. 50 mg samples of the left ventricle weighed and frozen. The samples were stored at −80 °C for not more than 1 month. For the sample preparation the tissues were crashed in liquid nitrogen, calculated amount (10 μl per mg tissue) of the buffer (10 mM Tris, 1 mM $MgCl_2$, 1 mM EDTA, 0.2 μM STI, 2 μM leupeptin, pH 7.4) added, homogenized at room temperature for 1 h with short shaking (Vortex in every 10–15 min, centrifuged at 15,000*g* for 4 min and the solid residual discarded. The obtained homogenate was supplemented by one-half (50 μl per 100 μl) of the sample buffer (0.2 M tris, 16% SDS, 1% DDT, 0.04% bromophenol blue, pH 6.8) and one-half of 50 % glycerol and incubated at 95 °C for 5 min. The HL-1 nonbeating cells were washed three times with 1 ml ice-cold phosphate buffered saline (PBS, 0.1 M KH_2PO_4, 0.15 M NaCl, pH 7.2) and lysed on ice with the Tris/Triton X-100 buffer (10 mM tris, 100 mM NaCl, 1 mM EDTA, 1 mM EGTA, 1% Triton X-100, 10% glycerol, 0.1% SDS, 0.5% sodium deoxycholate, pH 7.4), concentrated on 500 μl Vivaspin (10 000 MWCO PES) columns (Sartorius Stedim Biotech S.A.) up to approximately 100 μl, and supplemented by the sample buffer and treated as described above.

The protein concentration was routinely determined using the Pierce BCA Protein Kit as suggested by the manufacturer. Heating of the samples was performed at 60 °C for 30 min.

2.6. Western blotting

Electrophoresis was performed on the Mini Protean II from BioRad on 10% polyacrylamide gels in the Tris-tricine buffer solution developed by Schrägger and von Jagow [39] by applying of 0.5 μg (tubulin mixture) up to 300 μg of the tissue protein (tissue and cell lysates) as described in Fig. 1. The gels were fixed in 40% methanol and 5% phosphoric acid and, if required, stained with colloidal Coomassie G-250.

Blotting of the unstained gels was performed on the Trans-Blot SD Semi-Dry Transfer Cell (BioRad) using PVDF membranes (Millipore) according to the manufacturer's instructions. The blotting buffer contained 48 mM Tris, 39 mM glycine, 1% SDS and 20% methanol. The membranes were blocked for 1 hr with the skimmed milk/TBS solution (0.2 M Tris, 1.5 M NaCl, 0.1% Tween-20, 5% skimmed milk, pH 7.5) with gentle shaking and washed three times for 10 min with the same solution (without skimmed milk) and once in TBS solution lacking both the skimmed milk and Tween-20. Primary antibodies were diluted in the skimmed milk/TBS solution. Primary antibodies and used dalutions are shown in Table 1. Secondary antibodies were IgG and HRP-conjugated preparations. The membranes were exposed using the CL-X Posure film and SuperSignal West Dura Extended Duration substrate (SuperSignal West Dura Stable Peroxide Buffer and SuperSignal West Dura Luminol/Enhancer Solution).

Rabbit α-actinin antibody was obtained from Abcam (Abcam, ab82247). Mouse α-actinin antibody was obtained from Sigma

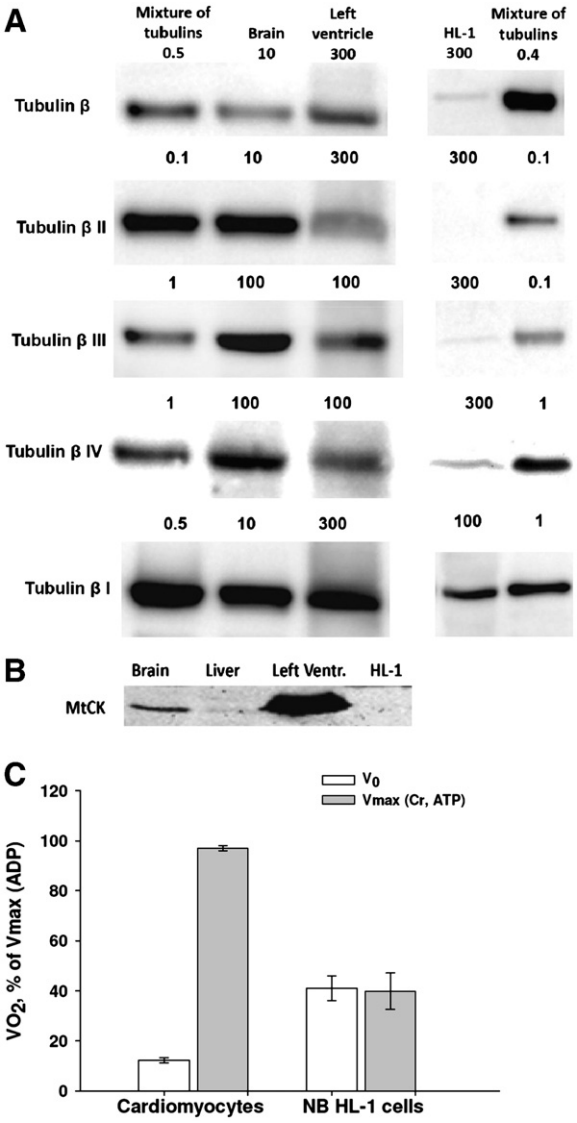

Fig. 1. Western Blot analysis of various tubulin isotypes (A) and MtCK (B) in different cells and tissues. LV—rat heart left ventricle. Numbers above the gel images show the amount of added total protein (in μg). Mixture of purified tubulins obtained from brain was used as a reference. The tubulin bands in reference samples correspond to the molecular mass of 55 kDa. (C) Creatine effect on the respiration of permeabilized cardiomyocytes and non-beating HL-1 cells. The rates are expressed as % of the maximal values (V_{max}) observed in the presence of ADP, 2 mM.

(A7811). VDAC antibody was obtained from the Laboratory of Physics and Structural Biology, National Institute of Child Health and Human Development, National Institute of Health, USA. Purified mixture of tubulin obtained as described before [16] was used as reference. They were kindly supplied by D. Sackett, Laboratory of Integrative and Medical Biophysics, Eunice Kennedy Shriver National Institute of Child Health and Human Development, National Institutes of Health, Bethesda, USA

2.7. Immunofluorescence

Freshly isolated cardiomyocytes and cultured cells were fixed in 4% paraformaldehyde at 37 °C for 15 min. After rinsing with PBS solution containing 2% BSA (bovine serum albumin) cells were permeabilized with 1% Triton X-100 at 25 °C for 30 min. Finally cells were rinsed repeatedly and incubated with primary antibody as described above for immunoblotting using concentrations indicated into the Table 1 (in 2% BSA containing PBS solution). The next day

Table 1
Primary antibodies.

Commercial name	Dilution for Western blot	Dilution for immunofluorescence	Immunogen
Mouse monoclonal βI Tubulin antibody, (Abcam ab11312)	1/20000	1/1000	Peptide corresponding to the C-terminal sequence
anti-tubulin βII(β2), (Abcam ab28036)	1/1000	1/1000	Amino acids CEEEEGEDEA at the C terminus
Rabbit polyclonal TUBB2A antibody, (Abnova PAB0379)		5 μg/ml	Amino acids DLVSEYQQYQDATADEQGE (417–435) at the C terminus
Rabbit monoclonal βIII Tubulin antibody, 5 (Abcam, ab52901	1/1000	1/50	Peptide corresponding to the C-terminal sequence
Mouse monoclonal βIV Tubulin antibody, (Abcam ab11315)	1/400	1/1000	Peptide corresponding to the C-terminal sequence
Rabbit polyclonal β Tubulin antibody, (Cell signalling 2146)	1/1000	1/50	Recognizes all tubulin isotypes

samples were rinsed and stained for 30 min at room temperature with secondary antibody. Secondary antibodies: Cy™ 5-conjugated Affini-Pure goat anti-mouse IgG (Jackson Immunoresearch 115-175-146), Goat polyclonal secondary antibody to mouse IgG-FITC (Abcam ab6785), goat anti-rabbit IgG, F(ab′)$_2$-FITC (Santa Cruz sc3839) were used respecting concentrations recommended by the providers. For co-staining the sequential protocol was applied. Two primary antibodies (one overnight at 4 °C and another for 2 h at room temperature) and two secondary antibodies were used to stain fixed samples with repeated rinsing procedures between every staining step. When the immunofluorescence was supplemented with mitochondria labeling, the fixed and immunostained cells (with primary and secondary antibodies) were incubated for 30 min at 37 °C in the presence of 2500 fold dilution of Mito-ID™ Red detection reagent (Mito-ID™ Red detection kit Enabling Discovery in Life Science, Enz-51007-500). For sharper image these cells were visualized immediately after labeling.

For the study of mitochondria arrangement in cardiomyocytes and HL-1 cells, freshly isolated or cultured cells were preloaded with mitochondria-specific fluorescent probe 0.2 μM MitoTracker Red™ and Green™ (Molecular Probes, Eugene, OR) for 2 h at 4 °C for cardiomyocytes and 15 min at 37° for HL-1 cells. Images were then analyzed using Volocity softwere (Improvision, France)

2.8. Confocal imaging

The fluorescence images were acquired with a Leica TCS SP2 AOBS inverted laser scanning confocal microscope (Leica, Heidelberg, Germany) equipped with a 63× water immersion objective (HCX PL APO 63.0×1.20 W Corr). Laser excitation was 488 nm for FITC and MitoTracker™ Green, 543 nm for Mito-ID™, and 633 nm for Cy 5, MitoTracker™ Red.

2.9. Measurements of oxygen consumption

The rates of oxygen uptake were determined with high-resolution respirometer Oxygraph-2K (OROBOROS Instruments, Austria) in Mitomed solution [25] containing 0.5 mM EGTA, 3 mM $MgCl_2$, 60 mM K-lactobionate, 3 mM KH_2PO_4, 20 mM taurine, 20 mM HEPES, 110 mM sucrose, 0.5 mM dithiothreitol (DTT), pH 7.1, 2 mg/ml fatty acid free BSA, complemented with 5 mM glutamate and 2 mM malate as respiratory substrates. Respiration was activated by addition of creatine to final concentration of 10 mM in the presence of ATP (2 mM). Maximal respiration rate was measured in the presence of ADP, 2 mM. Measurements were carried out at 25 °C; solubility of oxygen was taken as 240 nmol/ml [25].

2.10. Data analysis

The experiments were carried out independently in two different laboratories by using cardiomyocytes isolated from 10 animals. Functional data were expressed as means ± SE.

3. Results

In this study we analyze the distribution and possible functional roles of four isotypes of β-tubulins: βI (gene TUBB or TUBB5), βII (gene TUBB2A and TUBB2B), βIII (gene TUBIII), and βIV (gene TUBB4 and TUBB2C) in adult rat cardiomyocytes and mouse HL-1 cells (the classification of tubulin isotypes is based on recommended official names (http://www.ncbi.nlm.nih.gov/gene). Brain tissue samples and a mixture of tubulins purified from brain were used as a reference for each separate Western blot. Purified tubulins were obtained as described before (see Materials and methods) and were earlier used in the reconstitution experiments with isolated mitochondria [16]. Western blot analysis revealed the presence of all studied β-tubulin isotypes in rat left ventricular muscle tissue, as well as in brain and the reference mixture sample; in contrast, βII-tubulin was not detected in HL-1 cells (Fig. 1A). The distribution of the sarcomeric isoform of MtCK follows the same pattern of significant abundance in left ventricular muscle tissue and complete absence in cancer cells (Fig. 1B). This result is consistent with earlier data by Eimre et al. [36] who showed that in non-beating HL-1 cells the creatine kinase is presented by BB isozyme only. These results are in agreement with the observation that creatine maximally activates the respiration only

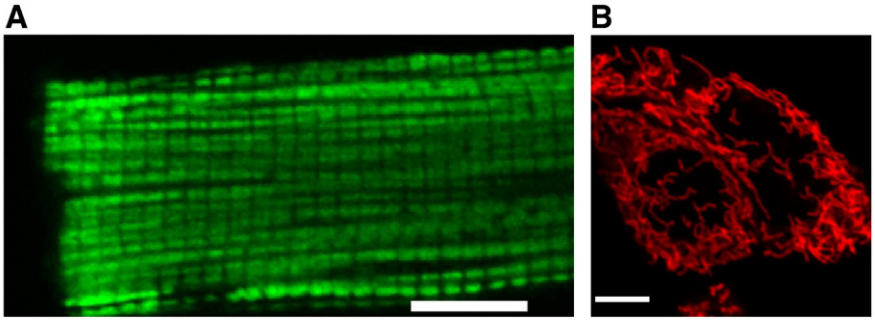

Fig. 2. Fluorescent microscopy imaging of mitochondria fluoroprobes, respectively. A: Mitochondria in cardiomyocytes visualized by fluorescent probe 0.2 μM MitoTracker™ Green shows separated individual organelles arranged in the regular lines. Scale bar 10 μm. B: Mitochondria in HL-1 cells 0.2 μM MitoTracker™ Red shows disorganized, filamentous mitochondrial network. Scale bar 6 μm.

in permeabilized cardiomyocytes and has no effect on respiration in permeabilized HL-1 cells (Fig. 1C).

The regular arrangement of individual mitochondria in adult cardiomyocytes imaged by MitoTracker green (Fig. 2A) dramatically contrasts with the disorganized thread-like mitochondrial reticulum of continuously dividing cancerous, highly glycolytic HL-1 cells (Mitotracker red, Fig. 2B). The striking differences observed in mitochondrial arrangement can obviously be related to the specific structural organization and mitochondria–cytoskeleton interactions in these cells [40].

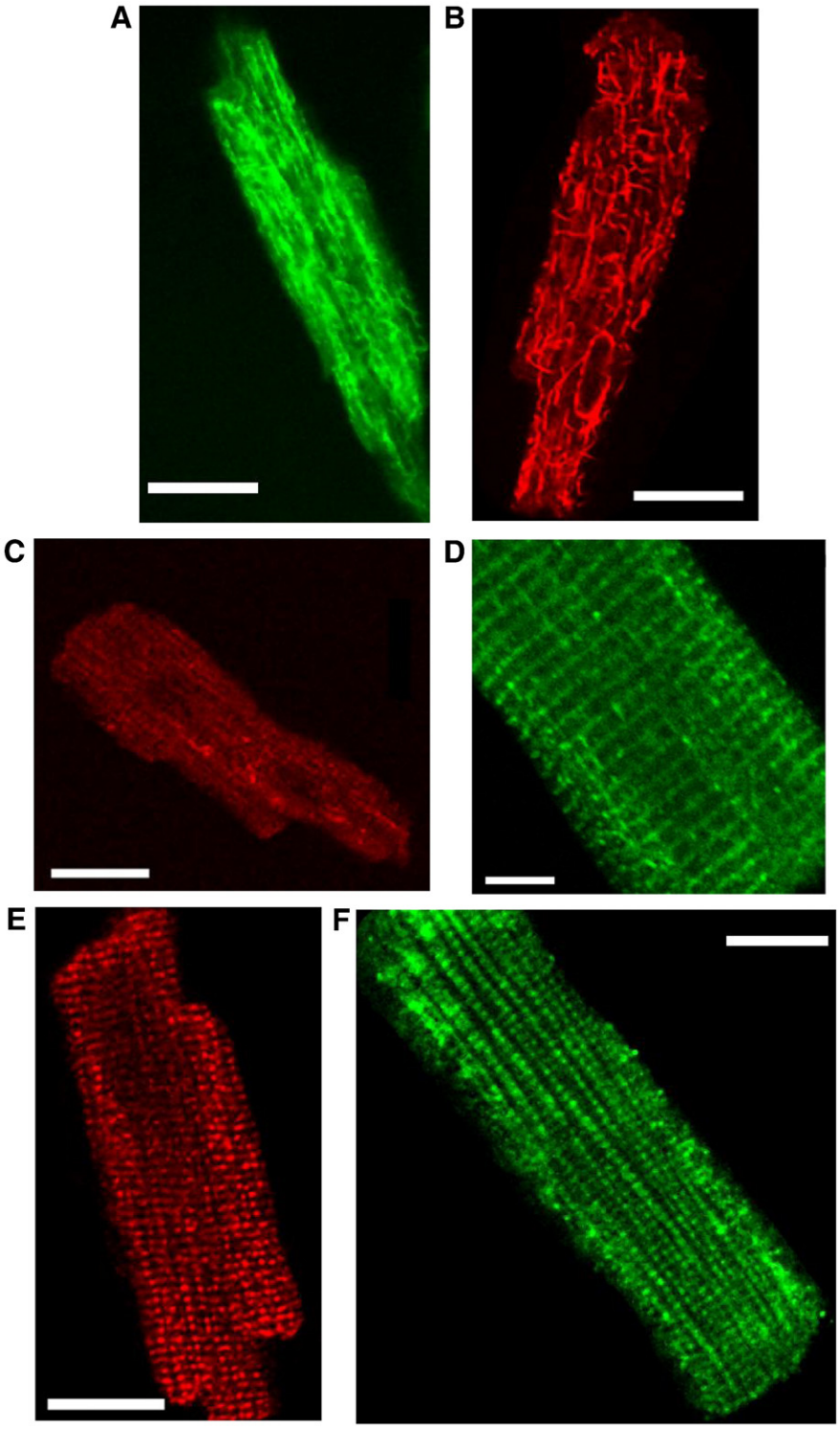

Fig. 3. Immunofluorescent confocal microscopy imaging of various β-tubulin isotypes in fixed cardiomyocytes. A: Longitudinally, obliquely and diffusely distributed total β-tubulins labeled with anti-β-tubulin antibody and FITC. Scale bar 24 μm. B: Tubulin labeled with anti-βIV-tubulin antibody and Cy5. βIV-tubulin shows polymerised longitudinally and obliquely oriented microtubules. Scale bar 21 μm. C: Diffusive intracellular distribution of tubulins labeled with anti-βI-tubulin antibody. Scale bar 10 μm. D: Tubulin labeled with anti-βIII-tubulin antibody and FITC demonstrates clearly distinguishable prevalent arrangement in transversal lines colocalized with sarcomeric Z-lines. Scale bar 6 μm. E: and F: Regularly arranged tubulins labeled with anti-βII-tubulin antibody and secondary antibodies: Cy5 (E) and FITC (F). In both cases, separate fluorescent spots organized in distinct longitudinally oriented parallel lines similarly to the mitochondrial arrangement (see Fig. 2A) in cardiomyocytes. Scale bar 14 μm (E) and scale bar 12 μm (F).

In order to further analyze the localization of β-tubulin isotypes, fixed cells were labeled first with primary antibodies against the proteins studied and then with fluorescent secondary antibodies (described in Materials and methods) and visualized by fluorescent confocal microscopy (Fig. 3). In control experiments without specific primary antibodies no binding of secondary fluorescent antibodies was seen (results not shown). Total β-tubulin forms tortuous microtubular structure with longitudinally and obliquely orientated crossed filaments in adult cardiomyocytes (Fig. 3A). The contribution of each individual tubulin isotype to these structures was analyzed by isotype-specific immunolabeling (Fig. 3B–F). The characteristic structure of β-tubulin appears to be mainly formed by polymerization of βIV-tubulin (Fig. 3B), whereas βI-tubulin is associated with a rather scattered distribution of fluorescent spots typical of its usual short polymerized fragments (Fig. 3C). βIII-tubulin is characteristically arranged in transversal lines demonstrating colocalization with sarcomeric Z-lines (Fig. 3D). This is very similar to earlier observation made using the immunogold labeling technique [18]. Thus both βIV-tubulin and βIII-tubulin appear at least partially responsible for the formation of the typical rod-like shape of adult cardiomyocytes.

The most interesting and exciting results of this study are related to the arrangement of βII-tubulin as revealed by differential immunofluorescent labeling (Cy5, Fig. 3E and FITC, Fig. 3F). In both cases, βII-tubulin is very regularly localized in rows along the long axis of the cell in an arrangement which is very similar to that of mitochondria (Fig. 2A). This observation is in a good agreement with the earlier findings of an association of β-tubulin with mitochondrial membranes using immunogold labeling [18]. Double-staining with anti-βII-tubulin and an anti-VDAC antibody against epitope 102–120, involved in the protein binding site, revealed an incomplete overlap of fluorescence (results not shown). This can be explained by the difficulties in immunolabeling VDAC, most probably due to presence of the bound tubulin resulting in a low accessibility of VDAC in cardiomyocytes.

Importantly, immunofluorescent labeling detects only traces of β-tubulin II in isolated mitochondria (Fig. 4A) in contrast to immunolabeled VDAC which is clearly detected in isolated mitochondria (Fig. 4B). This apparent contradiction can be explained by the fact that all cytoskeleton proteins associated with mitochondria are removed through trypsin proteolysis during their isolation.

By contrast with the results observed in cardiomyocytes, fluorescent immunolabeling of fixed HL-1 cells revealed the absence of βII-tubulin (Fig. 5A), confirming the results of Western blot analyses (Fig. 1). The clear colocalization of βIII-tubulin with α-actinin in Z-lines in cardiomyocytes is replaced by a rather diffusive distribution in HL-1 cells (Fig. 5B), which can be explained by the absence of the sarcomere structure in HL-1 cells. It is well known that overexpression of βIII-tubulin represents a valuable prognostic factor for the patients with aggressive evolution of ovarian, lung, pancreas, breast cancer and melanoma, and, at the same time, a poor probability of benefiting from the standard first-line platinum/taxane chemotherapy [41,42]. This suggests some interdependence between intracellular βIII-tubulin distribution and cancer metastasis. In addition, βI-tubulin labeling appears similar in cancerous HL-1 cells as in adult cardiac cells (Fig. 5C). The filamentous, bundle-like arrangement of βIV-tubulin in cancerous HL-1 cells (Fig. 5D) and the absence of a polymerized microtubular network could explain that they acquire a spherical shape in suspension and spread in culture.

The intracellular localization of βII-tubulin and βIII-tubulin isotypes was investigated by direct colocalization with Z-lines and mitochondria (Figs. 6 and 7). The Z-lines were labeled by α-actinin antibodies (Figs. 6A and 7A) for imaging of the sarcomere limits in cardiomyocytes. Labeling α-actinin with red fluorescence (Fig. 6A) and βIII-tubulin with green fluorescence (Fig. 6B) revealed significantly overlapping structures (Fig. 6C), suggesting that the previously observed specific transversal localization of β-tubulin is due to βIII-tubulin binding close to the Z-lines of the sarcomere.

Co-staining of α-actinin, labeled this time with a green fluorescence antibody (Fig. 7A) and mitochondria labeled by a specific red fluorescence probe Mito-ID™ (Fig. 7B) shows that mitochondria are localized very regularly between Z lines at the level of sarcomeres (see merged image in Fig. 7C). The absence of overlap of α-actinin at Z-lines and mitochondria-specific fluorescence reflects the absence of mitochondrial fusion. βII-tubulin labeling with green fluorescent antibodies shows its very regular localization in rows parallel to the long axis of the cell (Fig. 7D) orientated perpendicularly to Z-lines, an arrangement similar to that of mitochondria (Fig. 7E), and their full colocalization in cardiomyocytes (Fig. 7F). Comparison of the results displayed in Fig. 3E and F, and Fig. 7D and F indicates that all mitochondria are covered by βII-tubulin, which can therefore be used as an excellent natural intrinsic mitochondrial marker in adult cardiomyocytes.

In contrast, double labeling of HL-1 cells with antibodies against βII-tubulin (Fig. 8A) and with Mito-ID™ (Fig. 8B) as well as their overlap (Fig. 8C) clearly demonstrates the complete lack of βII-tubulin in cancerous HL-1 cells.

4. Discussion

Detailed comparative analysis of structure-function relationship in the regulation of energy fluxes in adult cardiomyocytes and cancerous HL-1 cells of cardiac phenotype described in our previous works [8,35–37] and in this study have yielded a wealth of information concerning the role of mitochondria–cytoskeleton interactions in shaping the specific pathway of energy transfer by the creatine kinase network in heart cells, as well as about the intracellular arrangement of mitochondria and complete prevention of their fusion in adult cardiomyocytes. These studies also show alteration of the mitochondrial dynamics, energy transfer pathways and metabolic phenotype in

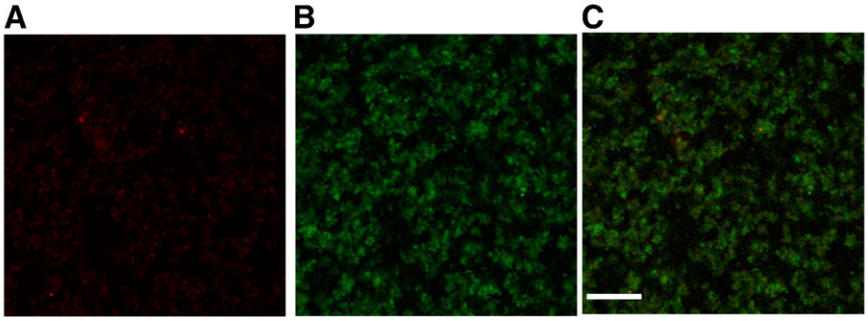

Fig. 4. Immunofluorescent confocal microscopy imaging of βII-tubulin and VDAC co-immunolabeling in isolated rat heart mitochondria. A: Absence of immunolabeling by anti-βII-tubulin (and Cy5) antibodies in isolated mitochondria. B: Strong immunofluorescent labeling of VDAC in isolated heart mitochondria (the interaction of mitochondria with βII-tubulin is removed by proteolysis with trypsin). C: The overlap of co-immunolabeling (βII-tubulin and VDAC). Scale bar 29 μm.

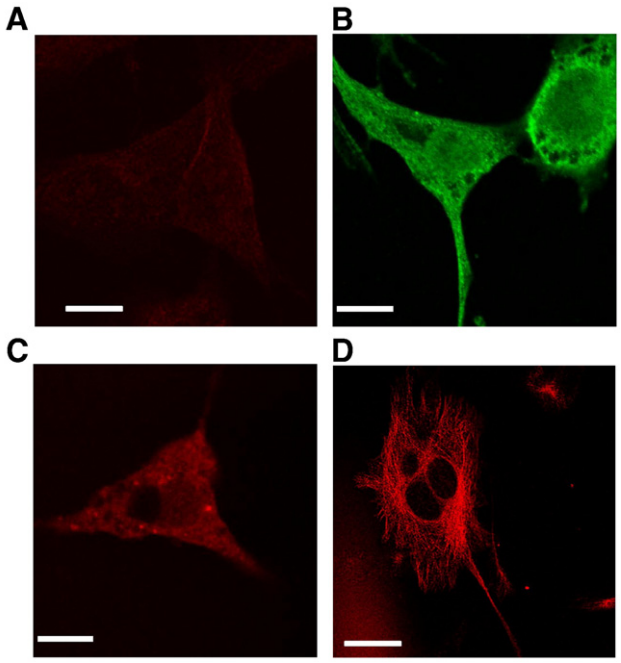

Fig. 5. Immunofluorescent confocal microscopy imaging of β-tubulin isotypes in fixed HL-1 cells. A: Tubulins labeled with mouse anti-βII-tubulin antibody and Cy5 are practically absent in HL-1 cells. Scale bar 14 μm. B: Tubulins labeled with anti-βIII-tubulin antibody and C: diffuse distribution of tubulins labeled with anti-βI-tubulin antibody. Scale bar 10 μm. D: Immunofluorescence imaging of polymerized tubulin microtubules labeled with anti-βIV-tubulin antibody and Cy5. The filaments show radial distribution from nucleus to cell periphery, creating also inter-connections between branches. Scale bar 18 μm.

cancerous cells that may help to understand the mechanism of the Warburg effect. In this study we found that different isotypes of tubulin have different intracellular distribution and therefore may play different roles in the control of energy fluxes and mitochondrial respiration in cardiac muscle cells. We have identified in adult cardiomyocytes the isotype of tubulin which is colocalized with mitochondria and is connected to the mitochondrial outer membrane–βII-tubulin. It is co-expressed with MtCK and by structural interactions with VDAC and ATP synthasome they form the mitochondrial interactosome [8,25,26]. This supercomplex, localized at contact sites of two mitochondrial membranes, is a key structure of a specific pathway of energy transport from mitochondria into the cytoplasm by phosphotransfer networks which effectively supply energy for contraction and ion pumps by local regeneration of ATP pools in myofibrils and at cellular membranes [8,25]. This prevents from wasting mitochondrial ATP in glycolytic reactions in spite of the presence of hexokinase-2 in the cytoplasm. βII-tubulin binding to the MOM may also protect the heart from apoptosis. On the contrary, in cancer cells of cardiac phenotype structural changes in the mitochondrial interactosome—lack of βII-tubulin, which is replaced by hexokinase-2, and lack of MtCK contribute to the mechanism of the Warburg effect by making possible the direct utilization of mitochondrial ATP for increased glucose phosphorylation and lactic acid production under aerobic conditions.

4.1. βII-tubulin isotypes in oxidative cardiomyocytes and glycolytic cancer HL-1 cells

Tubulin is one of the most representative proteins of cytoskeleton which among its other functions has a direct role in energy metabolism participating in the structuring of intracellular micro-compartments, formation of dissipative metabolic structures [43,44] and thus in the regulation of metabolic fluxes [45–49]. Under *in vivo* conditions cytoskeletal protein tubulin is highly dynamic and undergo rapid assembly/disassembly turnover by exchange of subunits. Building block of microtubules is a αβ-tubulin heterodimer [50]. In cardiomyocytes, about 70% of total tubulin is present in the polymerized form as microtubules whereas 30% occurs as non-polymerized cytosolic heterodimeric protein [51–54]. Interestingly, after complete dissociation of microtubular system by colchicine tubulin is still present in permeabilized cardiomyocytes, obviously because of its association with other cellular structures [55]. In higher vertebrates there are eight α-tubulin and seven β-tubulins encoded by different genes [50]. The majority of differences between tubulin isotypes are concentrated within the last 15 residues of the C-terminal (also called as isotype defining region) which is a main site for various alterations by post-translational modifications (PTMs) including tyrosinylation, acetylation, phosphorylation, polyglutamylation, and polyglycylation. In addition to that, C-terminal end has been identified to be a main target for numerous microtubule-associated proteins (MAPs) [56–58]. Differences in the C-terminal composition of tubulin isotypes determine the nature of PTM and affect their interactions with different cellular factors and the pattern of localization, thus explaining observations of this study. Recently, Rostovtseva et al. have proposed a mechanism of interaction between tubulin and VDAC, according to which the negatively charged carboxy-terminal tail (CTT) of tubulin penetrates into the cannel lumen interacting with a positively charged domain of VDAC [17,59]. For our experiments we used anti-βII-tubulin antibody against the CEEEEGEDEA amino acids of the CTT. The labeling of all mitochondria by this antibody shows that the negatively charged CTT of βII-tubulin is located on the outer mitochondrial membrane surface, very probably in close contact with positively charged region of the VDAC also located on this surface when it is in the closed conformation [60,61]. This explains also the decreased permeability of this channel for adenine nucleotides, as described below.

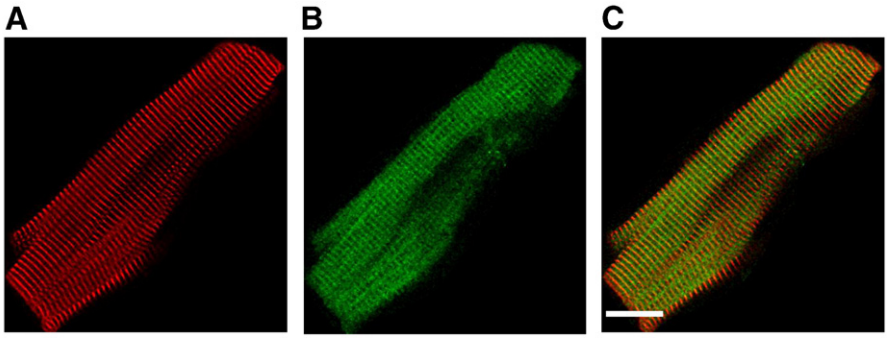

Fig. 6. Co-immunofluorescent labeling of α-actinin and βIII-tubulin in fixed cardiomyocytes. A: Characteristic sarcomeric transversal Z-lines labeled with anti-α-actinin antibody and Cy5. B: Tubulins labeled with anti-βIII-tubulin antibody and FITC. C: The overlap of α-actinin and βIII-tubulin. Both proteins are arranged at Z-lines. Scale bar 18 μm.

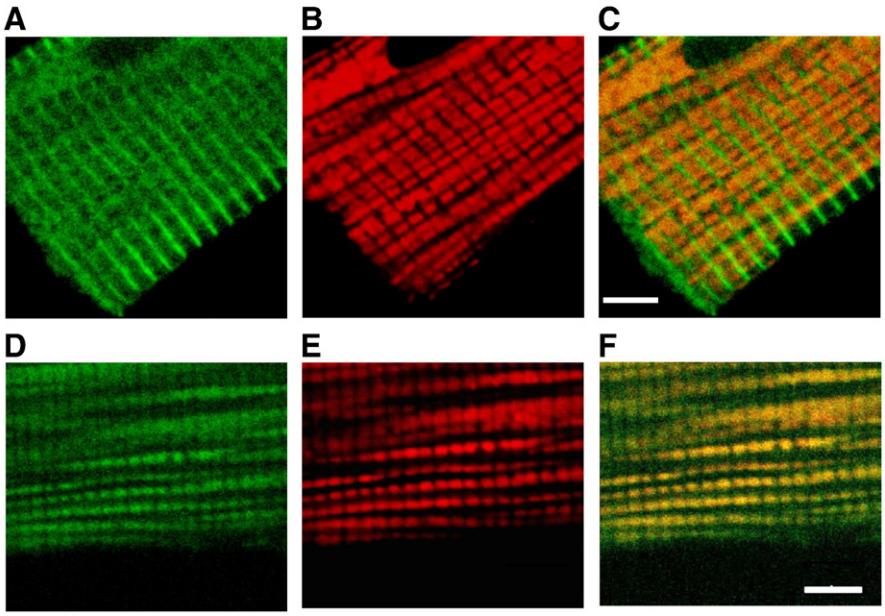

Fig. 7. Immunofluorescent imaging of α-actinin, β-tubulin II proteins and fluorescent staining of mitochondria. A: Green immunofluorescence of proteins labeled with anti-α-actinin antibody and FITC, demonstrating the characteristic sarcomeric transversal Z-lines. B: Typical regular arrangement of mitochondria labeled with Mito-ID™ Red. C: Merge image of A and B. Mitochondria (red) are localized exclusively between Z-lines (green). Scale bar 5 μm. D: Tubulins labeled with anti-βII-tubulin antibody and FITC. Fluorescent spots are regularly arranged (similarly to mitochondria). E: Mito-ID™ Red labeled mitochondria in cardiomyocyte. F: The overlap of D and E. β-tubulin class II (green) is arranged between Z-lines and fully co-localised with mitochondria. Scale bar 5 μm.

In contrast, we did not find βII-tubulin in cancer HL-1 cells of cardiac phenotype (Fig. 8). This observation matches well with previous finding of Hiser et al. [62]. Authors reported the absence of β-tubulin class II protein in 8 from 12 studied human cancer cell lines.

Mitochondria–cytoskeletal interactions, particularly the connection of βII-tubulin to the MOM may also prevent in significant degree the association of pro-apoptotic proteins to this membrane [63]. This may explain why apoptosis is rare in normal human hearts [64]. Possible alteration of mitochondria–tubulin interactions in dilated and ischemic cardiomyopathies may explain why the rate of apoptosis can increase several hundred folds in these diseases [64]. This is one of interesting problems for further study.

The presence of βII-tubulin at the outer mitochondrial membrane explains the very high value of apparent K_m for free exogenous ADP in adult permeabilized cardiomyocytes which is an order of magnitude higher than in isolated mitochondria (370 μM compared to 10–15 μM, respectively) [8,20–25]. Complete kinetic analysis of regulation of respiration by mitochondrial creatine kinase (MtCK) reaction in permeabilized cardiomyocytes confirmed the conclusions made in experiments with tubulin binding to VDAC [16,17,59] and uncovered specific restrictions of VDAC permeability by tubulin [25]. These experiments showed significant decrease of the apparent affinity for extramitochondrial ATP of MtCK localized on the outer surface of inner mitochondrial membrane in the intermembrane space in vivo in comparison with isolated mitochondria. This appears to be due to the diffusion restrictions created by interactions of VDAC in MOM with the tubulin αβ heterodimer [17,25,26,59]. Direct measurements of energy fluxes in permeabilized cardiomyocytes and in perfused hearts using the ^{18}O isotope tracer coupled with ^{31}P-NMR spectrometry showed that the ratio of the rates of PCr production to oxygen consumption ($VPCr/VO_2$) is close to 6, meaning that almost all energy is carried out of mitochondria by phosphocreatine molecules [26,65]. The results of these experimental studies showed that oxidative phosphorylation in cardiomyocytes is effectively regulated by creatine via MtCK in the mitochondrial interactosome (MI) [8,26].

In cancer HL-1 cells the apparent K_m for exogenous ADP was found to be in the range of 8–20 μM, which is similar to that of isolated mitochondria [35]. Moreover, in cancer cells creatine did not induce change of the respiration rates due to the absence of MtCK [35,36], but it was increased in cancer HL-1 cells in response to the addition of glucose showing its phosphorylation by hexokinase 2 [36].

Previous observations and results of the present study show that the two events—high apparent K_m for exogenous ADP and expression of MtCK correlate with the expression of βII-tubulin. The absence of

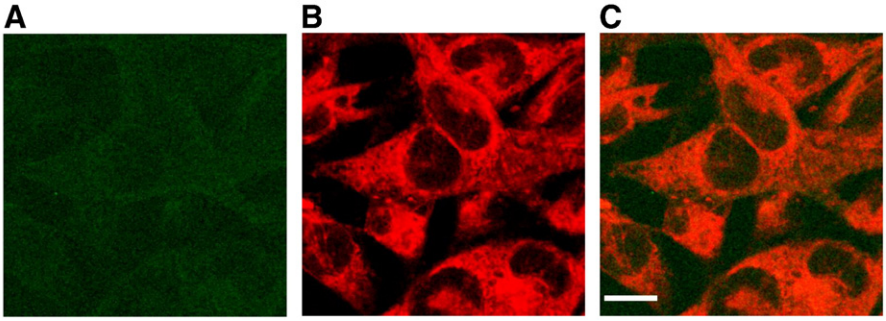

Fig. 8. The immunofluorescence of anti-βII-tubulin antibody (A) of rabbit source (and FITC) and mitochondria labeled with Mito-ID™ Red fluoroprobe (B) in HL-1 cells. Image A and merge image (C) shows the absence βII-tubulin labeling in HL-1 cells, scale bar 14 μm.

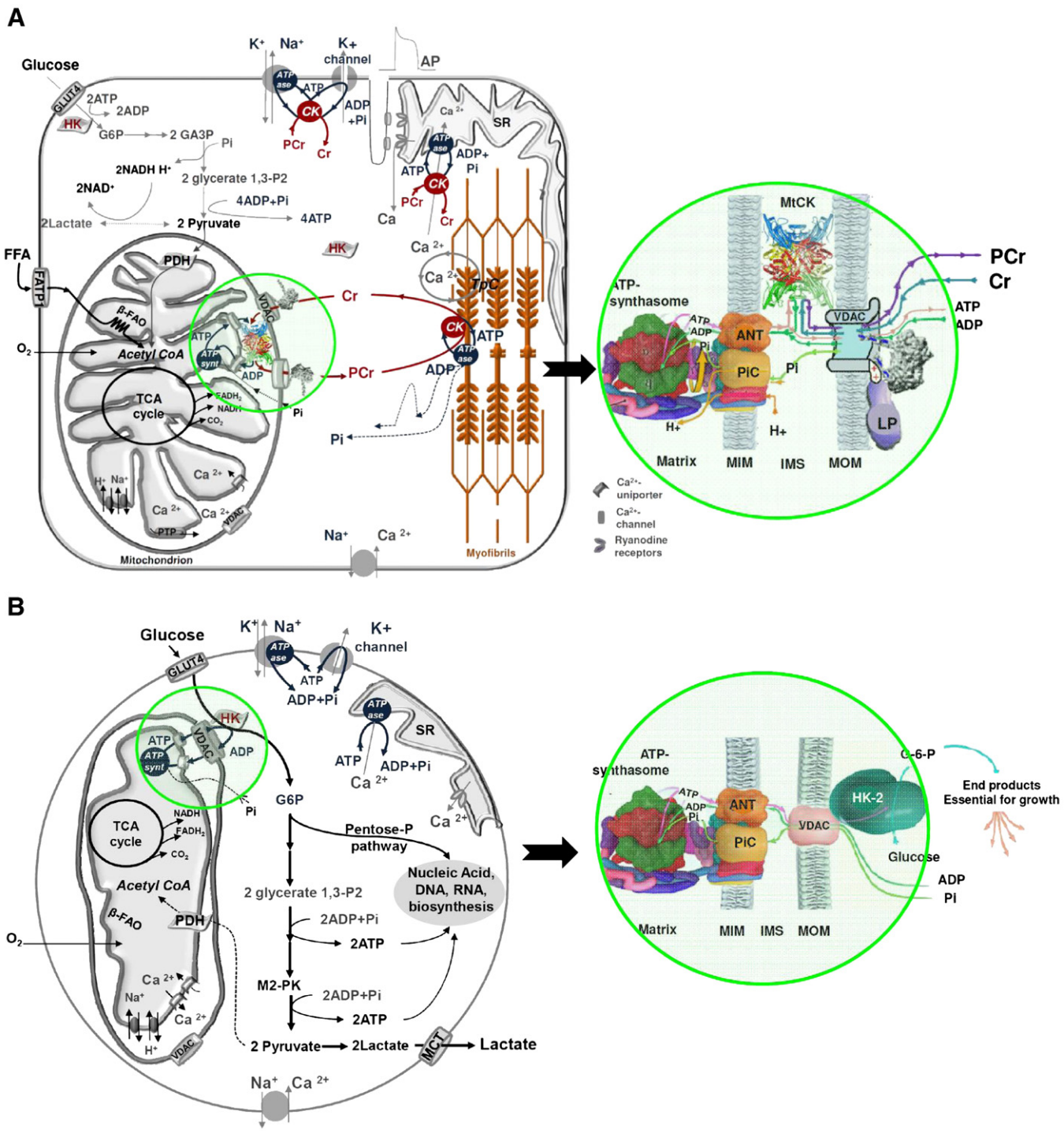

Fig. 9. Different pathways of intracellular energy transfer from mitochondria to cytoplasm in adult cardiomyocytes and HL-1 cells. A: Bessman–Wallimann–Saks pathway of energy transfer via creatine kinase phosphotransfer network in normal adult cardiomyocytes. Tubulin βII isotype is co-expressed with MtCK in Mitochondrial Interactosome and energy is channelled into cytoplasm by PCr which regenerate the local pools of ATP (phosphocreatine shuttle). Figure A represents adult cardiac cell (scheme at the left). Free fatty acids (FFA) are taken up by a family of plasma membrane proteins (FATP1), esterified to acyl-CoA which enters the β-oxidation pathway resulting in acetyl-CoA production. Glucose (GLU) is taken up by glucose transporter-4 (GLUT-4) and via the phosphorylation by hexokinase (HK) (depicted as soluble enzyme) with production of glucose-6-phosphate (G6P), enters the Embden–Meyerhof pathway. Pyruvate produced from glucose oxidation is transformed by the pyruvate dehydrogenise complex (PDH) into acetyl-CoA. G6P inhibits HK decreasing the rate of glucolysis. Acetyl-CoA is further oxidized to CO_2 in the tricarboxylic acids (TCA) cycle with the concomitant generation of NADH and $FADH_2$ which are oxidized in the respiratory chain (complexes I, II, III and IV) with final ATP synthesis. These pathways occur under aerobic conditions. Under anaerobic conditions, pyruvate can be converted to lactate. The insert shown in right panel illustrates functioning of Mitochondrial Interactosome (MI), a key system in energy transfer from mitochondria to cytoplasm. MI a supercomplex, formed by ATP synthase, adenine nucleotides translocase (ANT), phosphate carriers (PIC), mitochondrial creatine kinase (MtCK), voltage-dependent anion channel (VDAC) and bound cytoskeleton protein tubulin (specifically β-tubulin II selectively controlling VDAC permeability) and some linker proteins (LP), is responsible for recycling of ATP and ADP within mitochondria coupled to direct phosphorylation of creatine (Cr) into phosphocreatine (PCr). PCr is then transferred via cytosolic Cr/PCr shuttle to be used by functionally coupled CK with ATPases (acto-myosin ATPase and ion pumps) for regeneration of local ATP pools. B: Warburg–Pedersen pathway of energy transfer in cancer cells. Structure of mitochondrial interactosome is significantly modified: protein β-tubulin class II is replaced by HK, and the absence of MtCK allows all oxidative ATP to be exported directly from mitochondria. As the result, VDAC-bound HK is protected from the Glucose-6-P product inhibition, and uses mitochondrially produced ATP for phosphorylation of glucose and stimulation of glycolytic lactate production. The Glucose-6-P and glycolytic ATP synthesized during lactate production are used in biosynthetic pathways for cell growth and proliferation.

the βII-tubulin isotype both in isolated mitochondria and in HL-1 cells results in increase of the apparent affinity of oxidative phosphorylation for free ADP. This observation is consistent with the assumption that the binding of βII-tubulin to VDAC limits ADP/ATP diffusion through MOM.

The increased restriction of diffusion of adenine nucleotides through the MOM and the presence of MtCK functionally coupled to ANT in the MI are the most important mechanisms in the pathway of intracellular energy transport by phosphoryl transfer via the creatine kinase–phosphocreatine (PCr) network [3,8,9,66]. The system of compartmentalized creatine kinase isoenzymes and notably mitochondrial CK (MtCK) is the prerequisite condition for the efficient intracellular phosphotransfer [3]. The functioning of MI and its role in the energy transfer from mitochondria into the cytoplasm in cardiomyocytes with respiratory phenotype are represented schematically in Fig. 9A. In these cells, energy is transferred from mitochondria by the phosphotransfer PCr-CK circuit or shuttle. This pathway of energy transfer was in details described in Bessman [67,68], Wallimann [9,66] and Saks [3–8,21–26] laboratories and many others. In order to acknowledge the contribution of these three laboratories in the identification of energy transfer via creatine kinase phosphotransfer network it is named the Bessman–Wallimann–Saks pathway.

Analysis of the compartmentalized energy transfer by mathematical modelling [69] showed, in agreement with experimental data, that not more that 6–10% of ATP formed in oxidative phosphorylation is directly transferred out of mitochondria [70]. This, by maintaining local ATP pools, prevents the wasteful use of mitochondrial ATP for glucose phosphorylation by hexokinase-2, and ensures availability of an energy supply matching the specific cell needs (see Fig. 9A).

4.2. The lack of βII-tubulin and increased hexokinase-2 open the way to the Warburg effect

One of possible mechanisms triggering the Warburg effect is overexpression of hexokinase-2 [28,29,32,71–73]. In cancer cells, hexokinase-2 is bound to the VDAC and this interaction enhances its affinity for ATP by ~5-fold, and protects the enzyme from the inhibition by its byproduct glucose-6 phosphate [74]. In HL-1 cells hexokinase-2 is also overexpressed and its activity is increased by a factor of 5 in comparison with that observed in adult cardiomyocytes [36,37]. Thus, according to Pedersen's explanation of the Warburg mechanism, hexokinase-2 bound to VDAC actively phosphorylates glucose using mitochondrially synthesized ATP, redirecting it actively through the glycolytic pathway [28,75].

Hexokinase-2 is also prevalent in cardiac muscle cells [36,37,76]. However, it is only in cancer HL-1 cells which lack βII-tubulin, that hexokinase-2 binds to VDAC, altering cellular metabolism. Thus, binding of βII-tubulin to VDAC in normal cells prevents the wasting of mitochondrial ATP for increased lactate production that occurs in cancers cells through its binding of hexokinase-2 made possible by the absence of βII-tubulin. A comparative study of enzyme profiles in HL-1 cells and cardiomyocytes showed an increased activity of several glycolytic enzymes, particularly hexokinase-2 in HL-1 cells [37]. The decrease or absence of MtCK and the downregulation of its mRNA were previously reported in human sarcoma, gastric and colonic adenocarcinoma [77], indicating that these cells are unable to retain their intracellular creatine pool in the form of phosphocreatine because of the intrinsic low level of MtCK [77].

Thus, the mitochondrial interactosome in cancer HL-1 cells of cardiac phenotype is lacking of βII-tubulin and MtCK and significantly differs from that of healthy adult cardiac muscle cells incorporating ATP synthase, ANT, PiC, VDAC and HK-2 bound to VDAC. The absence of βII-tubulin and MtCK in the MI of HL-1 cells allows hexokinase-2 to bind to VDAC through its N-terminal hydrophobic domain [73]. The functioning of the MI in HL-1 cells is represented schematically in Fig. 9B. This pathway of energy transfer may be called the Warburg–Pedersen pathway to recognize the contribution of these distinguished investigators in its identification. In the absence of MtCK, mitochondrial ATP is directly carried out from mitochondria and used by VDAC-bound hexokinase-2 for glucose phosphorylation. Glucose-6P produced in this reaction enters the glycolytic and pentose-phosphate pathways, sustaining cellular growth and proliferation.

In conclusion, the remodelling of MI, namely the lack of βII-tubulin protein that makes possible hexokinase binding may be considered as the structural basis of the Warburg effect, explaining the switch from the energy transfer supporting the respiratory phenotype in normal cardiac cells to the more glycolytic phenotype of cancerous cells (see Fig. 9A and B). To verify this hypothesis, detailed further studies of distribution of hexokinase and tubulin isoforms in different cancer cells are needed.

Acknowledgments

The authors thank Dan L. Sackett, Laboratory of Integrative and Medical Biophysics, Eunice Kennedy Shriver National Institute of Child Health and Human Development, National Institutes of Health, Bethesda, USA, for reading this manuscript and for very helpful critical discussion. The authors thank Anu Nutt, National Institute of Chemical Physics and Biophysics, Tallinn, Estonia, for skilful technical assistance. This work was supported by INSERM, France, by Agence Nationale de la Recherche, project ANR-07-BLAN-0086-01 France, by grant No. 7823 from the Estonian Science Foundation, SF0180114Bs08 from Estonia Ministry of Education and Science, by National Council of Science and Technology of Mexico (CONACYT) and by a research grant from the Austrian Science Fund (FWF): [P 22080-B20].

References

[1] H.V. Westerhoff, A. Kolodkin, R. Conradie, S.J. Wilkinson, F.J. Bruggeman, K. Krab, J.H. van Schuppen, H. Hardin, B.M. Bakker, M.J. Mone, K.N. Rybakova, M. Eijken, H.J. van Leeuwen, J.L. Snoep, Systems biology towards life in silico: mathematics of the control of living cells, J. Math. Biol. 58 (2009) 7–34.
[2] R. Ramzan, K. Staniek, B. Kadenbach, S. Vogt, Mitochondrial respiration and membrane potential are regulated by the allosteric ATP-inhibition of cytochrome c oxidase, Biochim. Biophys. Acta 1797 (2010) 1672–1680.
[3] Molecular System Bioenergetics, in: V. Saks (Ed.), Energy for Life, Wiley-VCH: Weinheim, Gmbh, Germany, 2007.
[4] V. Saks, C. Monge, R. Guzun, Philosophical basis and some historical aspects of systems biology: from Hegel to Noble—applications for bioenergetic research, Int. J. Mol. Sci. 10 (2009) 1161–1192.
[5] V. Saks, The phosphocreatine-creatine kinase system helps to shape muscle cells and keep them healthy and alive, J. Physiol. 586 (2008) 2817–2818.
[6] V. Saks, T. Anmann, R. Guzun, T. Kaambre, P. Sikk, U. Schlattner, T. Wallimann, M. Aliev, M. Vendelin, The Creatine Kinase Phosphotransfer Network: Thermodynamic and Kinetic Considerations, the Impact of the Mitochondrial Outer Membrane and Modelling Approaches, in: M. Wyss, G. Salomons (Eds.), Creatine and Creatine Kinase in Health and Disease, Springer, Dordrecht, 2007, pp. 27–66.
[7] V. Saks, N. Beraud, T. Wallimann, Metabolic compartmentation—a system level property of muscle cells: real problems of diffusion in living cells, Int. J. Mol. Sci. 9 (2008) 751–767.
[8] V. Saks, R. Guzun, N. Timohhina, K. Tepp, M. Varikmaa, C. Monge, N. Beraud, T. Kaambre, A. Kuznetsov, L. Kadaja, M. Eimre, E. Seppet, Structure-function relationships in feedback regulation of energy fluxes in vivo in health and disease: mitochondrial interactosome, Biochim. Biophys. Acta 1797 (2010) 678–697.
[9] T. Wallimann, M. Wyss, D. Brdiczka, K. Nicolay, H.M. Eppenberger, Intracellular compartmentation, structure and function of creatine kinase isoenzymes in tissues with high and fluctuating energy demands: the "phosphocreatine circuit" for cellular energy homeostasis, Biochem. J. 281 (Pt 1) (1992) 21–40.
[10] Y. Capetanaki, R.J. Bloch, A. Kouloumenta, M. Mavroidis, S. Psarras, Muscle intermediate filaments and their links to membranes and membranous organelles, Exp. Cell Res. 313 (2007) 2063–2076.
[11] V.A. Saks, Z.A. Khuchua, E.V. Vasilyeva, O. Belikova, A.V. Kuznetsov, Metabolic compartmentation and substrate channelling in muscle cells. Role of coupled creatine kinases in in vivo regulation of cellular respiration—a synthesis, Mol Cell Biochem 133–134 (1994) 155–92.
[12] V.A. Saks, A.V. Kuznetsov, Z.A. Khuchua, E.V. Vasilyeva, J.O. Belikova, T. Kesvatera, T. Tiivel, Control of cellular respiration in vivo by mitochondrial outer membrane and by creatine kinase. A new speculative hypothesis: possible involvement of mitochondrial–cytoskeleton interactions, J. Mol. Cell. Cardiol. 27 (1995) 625–645.

[13] L. Winter, C. Abrahamsberg, G. Wiche, Plectin isoform 1b mediates mitochondrion-intermediate filament network linkage and controls organelle shape, J. Cell Biol. 181 (2008) 903–911.
[14] F. Bernier-Valentin, B. Rousset, Interaction of tubulin with rat liver mitochondria, J. Biol. Chem. 257 (1982) 7092–7099.
[15] M. Carre, N. Andre, G. Carles, H. Borghi, L. Brichese, C. Briand, D. Braguer, Tubulin is an inherent component of mitochondrial membranes that interacts with the voltage-dependent anion channel, J. Biol. Chem. 277 (2002) 33664–33669.
[16] C. Monge, N. Beraud, A.V. Kuznetsov, T. Rostovtseva, D. Sackett, U. Schlattner, M. Vendelin, V.A. Saks, Regulation of respiration in brain mitochondria and synaptosomes: restrictions of ADP diffusion in situ, roles of tubulin, and mitochondrial creatine kinase, Mol. Cell. Biochem. 318 (2008) 147–165.
[17] T.K. Rostovtseva, K.L. Sheldon, E. Hassanzadeh, C. Monge, V. Saks, S.M. Bezrukov, D.L. Sackett, Tubulin binding blocks mitochondrial voltage-dependent anion channel and regulates respiration, Proc. Natl. Acad. Sci. U. S. A. 105 (2008) 18746–18751.
[18] T. Saetersdal, G. Greve, H. Dalen, Associations between beta-tubulin and mitochondria in adult isolated heart myocytes as shown by immunofluorescence and immunoelectron microscopy, Histochemistry 95 (1990) 1–10.
[19] A.V. Kuznetsov, V. Veksler, F.N. Gellerich, V. Saks, R. Margreiter, W.S. Kunz, Analysis of mitochondrial function in situ in permeabilized muscle fibers, tissues and cells, Nat. Protoc. 3 (2008) 965–976.
[20] L. Kummel, Ca Mg-ATPase activity of permeabilised rat heart cells and its functional coupling to oxidative phosphorylation of the cells, Cardiovasc. Res. 22 (1988) 359–367.
[21] V.A. Saks, Y.O. Belikova, A.V. Kuznetsov, In vivo regulation of mitochondrial respiration in cardiomyocytes: specific restrictions for intracellular diffusion of ADP, Biochim. Biophys. Acta 1074 (1991) 302–311.
[22] V.A. Saks, E.V. Vassilyeva, Yu.O. Belikova, A.V. Kuznetsov, A. Lyapina, L. Petrova, N.A. Perov, Retarded diffusion of ADP in cardiomyocytes: possible role of outer mitochondrial membrane and creatine kinase in cellular regulation of oxidative phosphorylation, Biochim. Biophys. Acta 1144 (1993) 134–148.
[23] A.V. Kuznetsov, T. Tiivel, P. Sikk, T. Kaambre, L. Kay, Z. Daneshrad, A. Rossi, L. Kadaja, N. Peet, E. Seppet, V.A. Saks, Striking differences between the kinetics of regulation of respiration by ADP in slow-twitch and fast-twitch muscles in vivo, Eur. J. Biochem. 241 (1996) 909–915.
[24] F. Appaix, A.V. Kuznetsov, Y. Usson, L. Kay, T. Andrienko, J. Olivares, T. Kaambre, P. Sikk, R. Margreiter, V. Saks, Possible role of cytoskeleton in intracellular arrangement and regulation of mitochondria, Exp. Physiol. 88 (2003) 175–190.
[25] R. Guzun, N. Timohhina, K. Tepp, C. Monge, T. Kaambre, P. Sikk, A.V. Kuznetsov, C. Pison, V. Saks, Regulation of respiration controlled by mitochondrial creatine kinase in permeabilized cardiac cells in situ. Importance of system level properties, Biochim. Biophys. Acta 1787 (2009) 1089–1105.
[26] N. Timohhina, R. Guzun, K. Tepp, C. Monge, M. Varikmaa, H. Vija, P. Sikk, T. Kaambre, D. Sackett, V. Saks, Direct measurement of energy fluxes from mitochondria into cytoplasm in permeabilized cardiac cells in situ: some evidence for mitochondrial interactosome, J. Bioenerg. Biomembr. 41 (2009) 259–275.
[27] C. Chen, Y. Ko, M. Delannoy, S.J. Ludtke, W. Chiu, P.L. Pedersen, Mitochondrial ATP synthasome: three-dimensional structure by electron microscopy of the ATP synthase in complex formation with carriers for Pi and ADP/ATP, J. Biol. Chem. 279 (2004) 31761–31768.
[28] P.L. Pedersen, Warburg, me and Hexokinase 2: multiple discoveries of key molecular events underlying one of cancers' most common phenotypes, the "Warburg Effect," i.e., elevated glycolysis in the presence of oxygen, J. Bioenerg. Biomembr. 39 (2007) 211–222.
[29] P.L. Pedersen, Voltage dependent anion channels (VDACs): a brief introduction with a focus on the outer mitochondrial compartment's roles together with hexokinase-2 in the "Warburg effect" in cancer, J. Bioenerg. Biomembr. 40 (2008) 123–126.
[30] V. Gogvadze, B. Zhivotovsky, S. Orrenius, The Warburg effect and mitochondrial stability in cancer cells, Mol. Aspects Med. 31 (2010) 60–74.
[31] G. Kroemer, J. Pouyssegur, Tumor cell metabolism: cancer's Achilles' heel, Cancer Cell 13 (2008) 472–482.
[32] P.L. Pedersen, The cancer cell's "power plants" as promising therapeutic targets: an overview, J. Bioenerg. Biomembr. 39 (2007) 1–12.
[33] O. Warburg, On respiratory impairment in cancer cells, Science 124 (1956) 269–270.
[34] O. Warburg, K. Poesener, E. Negelein, Über den Stoffwechsel der Tumoren, Biochem. Z. 152 (1924) 319–344.
[35] T. Anmann, R. Guzun, N. Beraud, S. Pelloux, A.V. Kuznetsov, L. Kogerman, T. Kaambre, P. Sikk, K. Paju, N. Peet, E. Seppet, C. Ojeda, Y. Tourneur, V. Saks, Different kinetics of the regulation of respiration in permeabilized cardiomyocytes and in HL-1 cardiac cells. Importance of cell structure/organization for respiration regulation, Biochim. Biophys. Acta 1757 (2006) 1597–1606.
[36] M. Eimre, K. Paju, S. Pelloux, N. Beraud, M. Roosimaa, L. Kadaja, M. Gruno, N. Peet, E. Orlova, R. Remmelkoor, A. Piirsoo, V. Saks, E. Seppet, Distinct organization of energy metabolism in HL-1 cardiac cell line and cardiomyocytes, Biochim. Biophys. Acta 1777 (2008) 514–524.
[37] C. Monge, N. Beraud, K. Tepp, S. Pelloux, S. Chahboun, T. Kaambre, L. Kadaja, M. Roosimaa, A. Piirsoo, Y. Tourneur, A.V. Kuznetsov, V. Saks, E. Seppet, Comparative analysis of the bioenergetics of adult cardiomyocytes and nonbeating HL-1 cells: respiratory chain activities, glycolytic enzyme profiles, and metabolic fluxes, Can. J. Physiol. Pharmacol. 87 (2009) 318–326.
[38] V.A. Saks, G.B. Chernousova, D.E. Gukovsky, V.N. Smirnov, E.I. Chazov, Studies of energy transport in heart cells. Mitochondrial isoenzyme of creatine phosphokinase: kinetic properties and regulatory action of Mg2+ ions, Eur. J. Biochem. 57 (1975) 273–290.
[39] H. Schrägger, G. von Jagow, Tricine-sodium dodecyl-sulfate-polyacrylamide gel electrophoresis for the separation of proteins in the range from 1 to 100 kDa, Anal. Biochem. 166 (1987) 368–379.
[40] A.V. Kuznetsov, M. Hermann, J. Troppmair, R. Margreiter, P. Hengster, Complex patterns of mitochondrial dynamics in human pancreatic cells revealed by fluorescent confocal imaging, J. Cell. Mol. Med. (2009).
[41] K. Akasaka, C. Maesawa, M. Shibazaki, F. Maeda, K. Takahashi, T. Akasaka, T. Masuda, Loss of class III beta-tubulin induced by histone deacetylation is associated with chemosensitivity to paclitaxel in malignant melanoma cells, J. Invest. Dermatol. 129 (2009) 1516–1526.
[42] G. Raspaglio, I. De Maria, F. Filippetti, E. Martinelli, G.F. Zannoni, S. Prislei, G. Ferrandina, S. Shahabi, G. Scambia, C. Ferlini, HuR regulates beta-tubulin isotype expression in ovarian cancer, Cancer Res. 70 (2010) 5891–5900.
[43] I.M. de la Fuente, Quantitative analysis of cellular metabolic dissipative, self-organized structures, Int. J. Mol. Sci. 11 (2010) 3540–3599.
[44] I.M. De La Fuente, L. Martinez, A.L. Perez-Samartin, L. Ormaetxea, C. Amezaga, A. Vera-Lopez, Global self-organization of the cellular metabolic structure, PLoS ONE 3 (2008) e3100.
[45] M.A. Aon, S. Cortassa, Coherent and robust modulation of a metabolic network by cytoskeletal organization and dynamics, Biophys. Chem. 97 (2002) 213–231.
[46] M.A. Aon, B. O'Rourke, S. Cortassa, The fractal architecture of cytoplasmic organization: scaling, kinetics and emergence in metabolic networks, Mol. Cell. Biochem. 256–257 (2004) 169–184.
[47] L.M. Huff, D.L. Sackett, M.S. Poruchynsky, T. Fojo, Microtubule-disrupting chemotherapeutics result in enhanced proteasome-mediated degradation and disappearance of tubulin in neural cells, Cancer Res. 70 (2010) 5870–5879.
[48] B.G. Vertessy, F. Orosz, J. Kovacs, J. Ovadi, Alternative binding of two sequential glycolytic enzymes to microtubules. Molecular studies in the phosphofructokinase/aldolase/microtubule system, J. Biol. Chem. 272 (1997) 25542–25546.
[49] V. Saks, P. Dzeja, U. Schlattner, M. Vendelin, A. Terzic, T. Wallimann, Cardiac system bioenergetics: metabolic basis of the Frank–Starling law, J. Physiol. 571 (2006) 253–273.
[50] V. Redeker, Mass spectrometry analysis of C-terminal posttranslational modifications of tubulins, Methods Cell. Biol. 95 (2010) 77–103.
[51] S. Kostin, S. Hein, E. Arnon, D. Scholz, J. Schaper, The cytoskeleton and related proteins in the human failing heart, Heart Fail. Rev. 5 (2000) 271–280.
[52] J. Schaper, S. Kostin, S. Hein, A. Elsasser, E. Arnon, R. Zimmermann, Structural remodelling in heart failure, Exp. Clin. Cardiol. 7 (2002) 64–68.
[53] S. Hein, S. Kostin, A. Heling, Y. Maeno, J. Schaper, The role of the cytoskeleton in heart failure, Cardiovasc. Res. 45 (2000) 273–278.
[54] H. Tagawa, M. Koide, H. Sato, M.R. Zile, B.A. Carabello, G.T. Cooper, Cytoskeletal role in the transition from compensated to decompensated hypertrophy during adult canine left ventricular pressure overloading, Circ. Res. 82 (1998) 751–761.
[55] K. Guerrero, C. Monge, A. Bruckner, U. Puurand, L. Kadaja, T. Kaambre, E. Seppet, V. Saks, Study of possible interactions of tubulin, microtubular network, and STOP protein with mitochondria in muscle cells, Mol. Cell. Biochem. 337 (2010) 239–249.
[56] C. Janke, M. Kneussel, Tubulin post-translational modifications: encoding functions on the neuronal microtubule cytoskeleton, Trends Neurosci. 33 (2010) 362–372.
[57] R.F. Luduena, Multiple forms of tubulin: different gene products and covalent modifications, Int. Rev. Cytol. 178 (1998) 207–275.
[58] K.J. Verhey, J. Gaertig, The tubulin code, Cell Cycle 6 (2007) 2152–2160.
[59] T.K. Rostovtseva, S.M. Bezrukov, VDAC regulation: role of cytosolic proteins and mitochondrial lipids, J. Bioenerg. Biomembr. 40 (2008) 163–170.
[60] M. Colombini, VDAC: the channel at the interface between mitochondria and the cytosol, Mol. Cell. Biochem. 256–257 (2004) 107–115.
[61] M. Colombini, The published 3D structure of the VDAC channel: native or not? Trends Biochem. Sci. 34 (2009) 382–389.
[62] L. Hiser, A. Aggarwal, R. Young, A. Frankfurter, A. Spano, J.J. Correia, S. Lobert, Comparison of beta-tubulin mRNA and protein levels in 12 human cancer cell lines, Cell Motil. Cytoskeleton 63 (2006) 41–52.
[63] B. Antonsson, Mitochondria and the Bcl-2 family proteins in apoptosis signaling pathways, Mol. Cell. Biochem. 256–257 (2004) 141–155.
[64] G.W. Dorn II, Apoptotic and non-apoptotic programmed cardiomyocyte death in ventricular remodelling, Cardiovasc. Res. 81 (2009) 465–473.
[65] V. Saks, R. Favier, R. Guzun, U. Schlattner, T. Wallimann, Molecular system bioenergetics: regulation of substrate supply in response to heart energy demands, J. Physiol. 577 (2006) 769–777.
[66] T. Wallimann, M. Tokarska-Schlattner, D. Neumann, R.F. Epand, R.H. Andres, H.R. Widmer, T. Hornemann, V. Saks, I. Agarkova, U. Schlattner, The Phosphocreatine Circuit: Molecular and Cellular Physiology of Creatine Kinases, Sensitivity to Free Radicals, and Enhancement by Creatine Supplementation, in: V. Saks (Ed.), Molecular System Bioenergetics. Energy for Life, Wiley-VCH: Weinheim, GmbH, Germany, 2007, pp. 195–264.
[67] S.P. Bessman, C.L. Carpenter, The creatine–creatine phosphate energy shuttle, Annu. Rev. Biochem. 54 (1985) 831–862.
[68] S.P. Bessman, P.J. Geiger, Transport of energy in muscle: the phosphorylcreatine shuttle, Science 211 (1981) 448–452.
[69] M.K. Aliev, V.A. Saks, Compartmentalized energy transfer in cardiomyocytes: use of mathematical modeling for analysis of in vivo regulation of respiration, Biophys. J. 73 (1997) 428–445.
[70] R. Guzun, V. Saks, Application of the principles of systems biology and Wiener's cybernetics for analysis of regulation of energy fluxes in muscle cells in vivo, Int. J. Mol. Sci. 11 (2010) 982–1019.

[71] P.L. Pedersen, Transport ATPases into the year 2008: a brief overview related to types, structures, functions and roles in health and disease, J. Bioenerg. Biomembr. 39 (2007) 349–355.
[72] P.L. Pedersen, Y.H. Ko, S. Hong, ATP synthases in the year 2000: evolving views about the structures of these remarkable enzyme complexes, J. Bioenerg. Biomembr. 32 (2000) 325–332.
[73] P.L. Pedersen, S. Mathupala, A. Rempel, J.F. Geschwind, Y.H. Ko, Mitochondrial bound type II hexokinase: a key player in the growth and survival of many cancers and an ideal prospect for therapeutic intervention, Biochim. Biophys. Acta 1555 (2002) 14–20.
[74] E. Bustamante, H.P. Morris, P.L. Pedersen, Energy metabolism of tumor cells. Requirement for a form of hexokinase with a propensity for mitochondrial binding, J. Biol. Chem. 256 (1981) 8699–8704.
[75] S.P. Mathupala, Y.H. Ko, P.L. Pedersen, Hexokinase-2 bound to mitochondria: cancer's stygian link to the "Warburg Effect" and a pivotal target for effective therapy, Semin. Cancer Biol. 19 (2009) 17–24.
[76] J.E. Wilson, Hexokinases, Rev. Physiol. Biochem. Pharmacol. 126 (1995) 65–198.
[77] S. Patra, S. Bera, S. SinhaRoy, S. Ghoshal, S. Ray, A. Basu, U. Schlattner, T. Wallimann, M. Ray, Progressive decrease of phosphocreatine, creatine and creatine kinase in skeletal muscle upon transformation to sarcoma, FEBS J. 275 (2008) 3236–3247.